SYMMETRICAL VIEWPOINT REPRESENTATIONS IN FACE-SELECTIVE REGIONS CONVEY AN ADVANTAGE IN THE PERCEPTION AND RECOGNITION OF FACES

Tessa R. Flack[1,2], Richard J. Harris[3], Andrew W. Young[1] & Timothy J. Andrews[1]

[1] Department of Psychology, University of York, YO10 5DD

[2] School of Psychology, University of Lincoln, LN6 7TS

[3] School of Psychology, University of Leeds, LS2 9JT

Figures: 5

Tables: 4

Abstract: 247

Introduction: 652

Discussion: 1665

Corresponding author: timothy.andrews@york.ac.uk

Key words: face, viewpoint, symmetry, view-invariance

ABSTRACT

Learning new identities is crucial for effective social interaction. A critical aspect of this process is the integration of different images from the same face into a view-invariant representation that can be used for recognition. The representation of symmetrical viewpoints has been proposed to be a key computational step in achieving view-invariance. The aim of this study was to determine whether the representation of symmetrical viewpoints in face-selective regions is directly linked to the perception and recognition of face identity. In Experiment 1, we measured fMRI responses while male and female human participants viewed images of real faces from different viewpoints (-90^o, -45^o, 0^o, 45^o, 90^o from full-face view). Within the face regions, patterns of neural response to symmetrical views (-45^o & 45^o or -90^o & 90^o) were more similar than responses to non-symmetrical views in the FFA and STS, but not in the OFA. In Experiment 2, participants made perceptual similarity judgements to pairs of face images. Images with symmetrical viewpoints were reported as being more similar than non-symmetric views. In Experiment 3, we asked whether symmetrical views also convey an advantage when learning new faces. We found that recognition was best when participants were tested with novel face images that were symmetrical to the learning viewpoint. Critically, the pattern of perceptual similarity and recognition across different viewpoints predicted the pattern of neural response in face-selective regions. Together, our results provide support for the functional value of symmetry as an intermediate step in generating view-invariant representations.

SIGNIFICANCE STATEMENT

The recognition of identity from faces is crucial for successful social interactions. A critical step in this process is the integration of different views into a unified, view-invariant representation. The representation of symmetrical views (e.g. left profile and right profile) has been proposed as an important intermediate step in computing view-invariant representations. We found view symmetric representations were specific to some face-selective regions, but not others. We also show that these neural representations influence the perception of faces. Symmetric views were perceived to be more similar and were recognized more accurately than non-symmetric views. Moreover, the perception and recognition of faces at different viewpoints predicted patterns of response in those face regions with view symmetric representations.

INTRODUCTION

Faces are seen from many different angles in everyday life and differences in viewpoint play an important role in social perception. For example, different orientations provide useful information about internal mental states, such as the focus of attention, and they directly affect social attributions (Sutherland et al., 2017). However, changes in viewpoint make the process of face recognition more difficult, because so many different views can be generated from the same identity. Despite this challenge, we can recognise familiar faces from different viewpoints with relative ease (Hancock et al,, 2000), raising the critical theoretical question of how this viewpoint-invariance for recognising familiar faces is achieved (Young, 2018; Young & Burton, 2017). Cognitive models of face processing have suggested that the recognition of facial identity is based on a view-invariant representation that receives convergent input from relatively viewpoint-specific representations (Bruce & Young, 1986; Burton et al., 1999; although see Tarr and Bulthoff, 1998). Understanding how the brain generates this viewpoint invariant representation is central to understanding how we recognize faces.

Neurophysiological studies have shown that neurons in the temporal lobe can be selective for different facial viewpoints (Perrett et al., 1991). This led to the idea that recognition is initially based on multiple viewpoint-specific representations that are a precursor to viewpoint-invariant representations of identity (Perrett et al., 1998). However, these studies also reported a sub-population of neurons that showed bimodal responses in which there was selectivity to two different viewpoints, typically symmetrical viewpoints. More recently, Freiwald and Tsao (Freiwald & Tsao, 2010; Dubois et al., 2015) used fMRI in combination with single neuron recording in different face regions of the monkey temporal

lobe. They found that in the most posterior face regions (ML/MF), neurons were selective for the viewpoint of the face. However, a more anterior face patch (AL) contained neurons that showed mirror-symmetric tuning for viewpoint. The most anterior region (AM) contained view-invariant neurons.

Neuroimaging studies have also found evidence for the representation of viewpoint symmetry in face-selective regions of the human brain. Early studies found viewpoint-selective responses to unfamiliar faces in face-selective regions (Andrews & Ewbank, 2004; Carlin et al., 2011; Fang et al., 2007; Grill-Spector et al., 1999; Guntupalliet al., 2017; Weibert et al., 2018), with partial view-invariance (20 – 30°) for familiar faces (Eger, Schweinberger et al., 2005; Ewbank & Andrews, 2008; Pourtois et al., 2005). More recently, a number of studies have found selectivity to mirror-symmetric viewpoints in face-selective regions (Axelrod & Yovel, 2012; Guntupalli et al., 2017; Kietzmann et al., 2012; 2015, 2017). These studies found that the pattern of response in face regions was more similar for symmetrical views of the face compared to non-symmetrical views. However, the existence of mirror-symmetric representations in face regions has been challenged by reports maintaining that patterns of response can be better explained by view-dependent representations (Ramírez, 2018; Ramirez et al., 2014).

The existence and location of mirror-symmetric representations of faces is important, because they are often thought to form a key computational step in the generation of viewpoint-invariant representations (Axelrod & Yovel, 2012; Freiwald & Tsao, 2010; Kietzmann et al., 2012). The aim of this study was to determine where mirror-symmetric representations exist and whether there is a direct link with the perception and recognition of faces. Previous behavioural studies using face matching tasks have found

99 better performance on face image pairs showing symmetrical compared to non-symmetrical
100 viewpoints (Busey & Zaki, 2004; Troje & Bülthoff, 1998). Here, we used perceptual matching
101 and face-learning paradigms to ask whether mirror-symmetric representations in face-
102 selective regions can be predicted by performance on such behavioural tasks. A key feature
103 of our study is the use of real human faces, as opposed to computer generated faces.
104 Human faces are not perfectly mirror symmetrical, so it is important to use real human faces
105 to determine if the brain represents symmetry in the real world and whether these
106 representations are important for the perception and recognition of identity.

METHOD

Participants

All participants had normal or corrected-to-normal vision with no history of neurological conditions. 20 right-handed participants (10 female, mean age 25.3 ± 3.1) took part in Experiment 1. 20 participants took part in Experiment 2 (12 female, mean age 24.2 ± 3.6). 48 participants took part in Experiment 3 (37 female, mean age 23.2 ± 5.2). Written consent was obtained from all participants and the studies were approved by the York Neuroimaging Centre Research Ethics Committee (Exp. 1), the Department of Psychology Ethics Committee at the University of York (Exp. 2) and Durham University (Exp. 3). All experiments conformed to the principles of the Declaration of Helsinki.

Experiment 1

Experimental Design

Face images were taken from the Radboud Faces Database (Langner et al., 2010). There were five stimulus conditions, presented in a block design: 1) right profile (-90^{o}), 2) right ¾ profile (-45^{o}), 3) front view (0^{o}), 4) left ¾ profile (45^{o}), 5) left profile (90^{o}). These viewpoints were shown across 5 different identities (Figure 1). Images were placed onto a 1/f amplitude mask to ensure that all images stimulated the same amount of the visual field despite changes in viewpoint.

Images from each viewpoint condition were presented in a blocked design. Each block contained 5 images (columns in Fig. 1), with each image presented for 1 sec followed by a 200 msec grey screen. There was a 9 sec inter-block period during which a grey fixation screen was presented. Each viewpoint condition was repeated 6 times, giving a total of 42 blocks. The order of identities in each block was randomized across blocks. To ensure

participants were paying attention during the scan, participants were required to monitor the images and indicate using a response box when they saw a red dot superimposed onto one of the images. Accuracy on this task was very high (99.9 ± 0.5%).

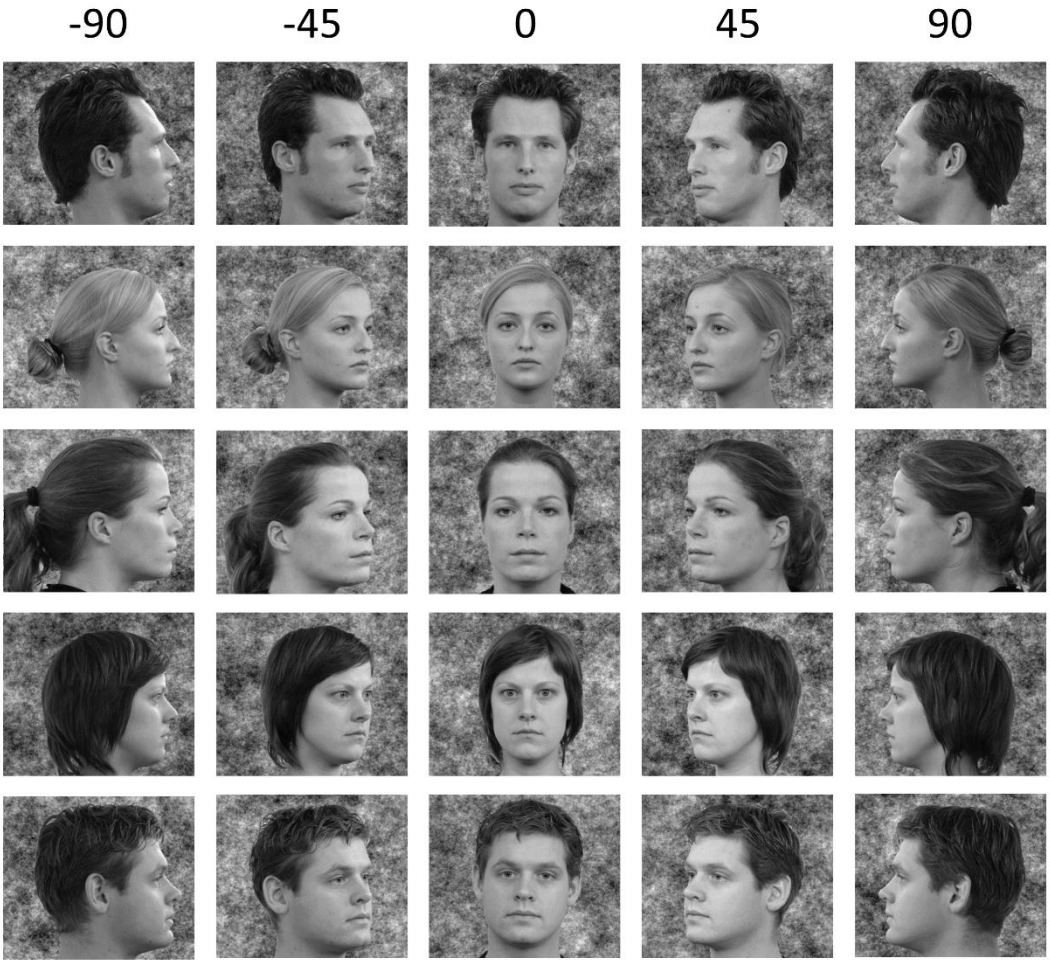

Figure 1 Examples of stimuli from Experiment 1. Each column shows the sequence of images in a representative stimulus block for the different conditions. Within each block the viewpoint remained the same, with the identity varying across images.

Imaging Parameters

Data for Experiment 1 were collected using a GE 3 Tesla HD Excite MRI system with an eight channel phased array head coil tuned to 127.4MHz. A gradient echo planar imaging (EPI) sequence was used to acquire the data. The acquisition parameters were: 38 contiguous axial slices, repetition time (TR) 3 seconds, echo time (TE) 32.5 milliseconds, flip angle 90°,

field of view (FOV) 28.8 x 28.8 cm, matrix 128 x 128, slice-thickness 3mm, voxel size 2.25 x 2.25 x 3mm. To improve registration, the EPI image was co-registered with a T1-weighted image taken in the same plane, before being registered to the high resolution main structural scan (T1-weighted, 1.13 x 1.13 x 1 mm) of each participant. This was then co-registered to the standard MNI 152 brain.

fMRI Analysis

Our main analysis focussed on face-selective regions (fusiform face area: FFA, occipital face area: OFA; superior temporal sulcus: STS, inferior frontal gyrus: IFG; amygdala: AMG). There were two important principles underlying the way in which we defined the face-selective regions of interest (ROIs). The first principle was that ROIs should be based on independent data. Given that we were investigating the reliability of patterns of response across individuals, it was essential that these came from independent participants. The second principle was that ROIs must be of the same size (number of voxels), to allow the MVPA analyses to have comparable potential power to detect underlying patterns of response in each region.

An independent localiser scan was therefore used to define group level ROIs using different participants (n = 83). Responses to faces that varied in identity and viewpoint were compared to the response to scrambled faces. ROIs comprised of the 500 most significant voxels in the OFA, FFA and STS (Sormaz, Watson, Smith, Young, & Andrews, 2016). Our analysis was supplemented by using ROIs based on probabilistic visual field maps developed by Wang and colleagues (Wang, Mruczek, Arcaro, & Kastner, 2015). Our rationale for using these masks was to determine how the representation of face viewpoint changes from early

to higher levels of the visual system. The size of each region in our analysis is shown Table 1-4.

Pattern analyses were performed using the PyMVPA toolbox (http://www.pymvpa.org/; Hanke et al., 2009). Parameter estimates from a univariate analysis of the main experiment were first normalised by subtracting the average response across the five viewpoint conditions (-90°, -45°, 0°, 45°, 90°). The reliabilities of the neural patterns of response were then determined using a modified form of the correlation-based MVPA method devised by Haxby and colleagues (Haxby et al., 2001), whereby patterns of response from each participant were compared to the patterns resulting from the group analysis with that participant left out. This Leave One Participant Out method (LOPO) allowed us to determine the consistency of the patterns of response across participants by measuring how similar each participant's responses were to those for the rest of the group. This method has been successfully used in several recent studies from our research group (Coggan, Liu, Baker, & Andrews, 2016; Rice, Watson, Hartley, & Andrews, 2014; Watson, Hartley, & Andrews, 2014; Weibert et al., 2018). The group pattern was derived by entering all but one of the participants' data into a higher-level group analysis (mixed effects, FLAME http://www.fmrib.ox.ac.uk/fsl). This group pattern of response for each condition was then correlated with the pattern from the participant who was omitted from the group. For each unique pair of conditions, the LOPO method was repeated 20 times, with a different participant being omitted from the rest of the group each time. A Fisher's Z-transformation was then applied to the correlations prior to statistical analysis.

To assess whether there were distinct patterns of response to individual viewpoint directions, paired t-tests were used to test the difference between the average within-

187 condition (e.g. -90^{o} vs -90^{o}, -45^{o} vs -45^{o}) and the corresponding between-condition
188 correlations. If a viewpoint evoked a distinct pattern of response, then the within-condition
189 correlations for the individual participant and rest of the group data should be higher than
190 the between-condition correlations in the given region.

191 Next, a representational similarity analysis (Kriegeskorte, Mur, & Bandettini, 2008)
192 was performed to determine how information about viewpoint was represented. We
193 compared the fit achieved by 3 models derived from different theoretical perspectives: 1)
194 Viewpoint, 2) Direction and 3) Symmetry. In the Viewpoint model the value of each cell was
195 proportional to the degree of difference in rotation between viewpoints. In the Direction
196 model, cells involving combinations of viewpoints with the same direction (both-left facing
197 or both right-facing) were given the value 1, whereas all other cells were coded 0. In the
198 Symmetry model, cells showing symmetrical viewpoints were given a value of 1 and non-
199 symmetrical viewpoints were given a value 0. To prevent differences in the overall
200 magnitude of within-condition and between-condition correlations artificially inflating
201 differences in correlations between matrices, our analysis was only performed on the
202 between-cluster comparisons. All models were normalized using a Z-transform (mean = 0,
203 SD = 1) and then used in a linear regression analysis, with the outcomes defined as the
204 correlation matrices obtained from the MVPA concatenated across LOPO iterations. For
205 each model, elements within the matrix were extracted and flattened to a vector. These
206 vectors were then repeated and tiled to match the number of participants. For each
207 participant, correlation matrices were extracted and flattened to a vector. These vectors
208 were then concatenated and entered into the model as the outcome variable. This analysis
209 yielded a regression coefficient and an error that reflected variance across participants. All

regression analyses included a constant term. From this analysis, it was possible to determine the relative fit to each model in each ROI.

Experiment 2

Stimuli and Experimental Design

To determine whether symmetrical viewpoints were seen as being more similar than non-symmetrical viewpoints, we conducted a behavioural study in which participants rated the perceptual similarity of pairs of images which varied in viewpoint. Stimuli consisted of the same greyscale images used in Experiment 1. Images were presented in pairs, with the identity across the two images remaining the same, but the viewpoint changing. Images were presented sequentially, with the first image being presented for 1 sec, a 200 msec ISI and then the second image. Each viewpoint was presented with every other viewpoint, in both the first and second position. For each identity, there were 2 trials for each of the 10 viewpoint combinations. This was repeated for each of the 5 identities, giving a total of 10 trials for each of the 10 viewpoint combinations. The order of trials was randomised for each individual participant. Participants were required to respond with a button press indicating how similar they perceived the images to be, on a scale of 1 – 7 (1 being less similar and 7 being more similar). Participants were given an unlimited time to respond. The perceptual similarity between symmetric and non-symmetric responses was compared using a paired t-test. The perceptual similarity between different viewpoints was then used as a model in a regression analysis of the fMRI data from different regions.

Experiment 3

Stimuli and Experimental Design

Experiment 3 used a face-identity learning paradigm (see Longmore, Liu, and Young, 2008) to determine if a face learnt in one viewpoint conveyed an advantage in the recognition of the symmetrical viewpoint. Faces from the Radboud database were again used in this experiment. There were 20 male identities each posing a neutral facial expression at the following viewpoints: -90°, -45°, 0°, 45°, 90°. The 20 identities were split into two sets. Participants were randomly assigned to Set 1 or Set 2. Within each set, each of the 10 identities was assigned to one of the five viewpoints. The assignment of identities to viewpoints was randomized for each participant. This generated 10 face images: 2 images for each viewpoint.

In the learning phase, participants were presented with these 10 face images. The faces were presented sequentially, with each face being presented for 5 seconds, with a 500ms ISI between each trial. Underneath each face was a first name. Names were randomly assigned to faces for each participant from a set of 10 names. These names were chosen to be short and common in the UK, consisting of one or two syllables and three or four letters, e.g. Paul, Tim. Participants were instructed to remember the face and its corresponding name.

In the training phase, the 10 faces were split into two blocks of 5 faces. Participants were presented with the first block of 5 faces. These faces were presented individually, and for an unlimited time. Participants were asked to pick the name that they believed belonged to the face. The five name options were displayed below the face and participants had to use the mouse to click on the name they thought matched the face. The order of the names

was random for each participant. Once a response had been recorded, participants were given feedback to indicate whether they were correct or not. If they were incorrect, they were told what the correct name was for the target face. This feedback was provided to aid and reinforce the learning in this training phase. In order to move to the next block of 5 faces, the participants had to correctly name each face twice in a row. For example, if a given face was named correctly once, and then incorrectly the next time it was presented, the correct count for this face was returned to 0 and the participant had to complete two more trials correctly in a row, in order to continue. Once the participant had correctly named the face twice in a row, it was removed from the block. This process was repeated with the remaining block of five faces. Next, the entire set of 10 faces were presented. In this final block of the training phase, participants had to correctly name all 10 faces twice in a row (in the same way as described above) in order to complete the phase.

In the final test phase of the experiment, participants were presented with all images from the set. This included the 10 images used for training and the remaining 40 images that were not used during training. Images were presented twice, giving 100 trials. The task was to match the name to the face from the 10 names displayed underneath the face. Feedback was not given in this phase of the experiment. For each identity, the aim was to determine if the (untrained) face images that were symmetrical to the trained view were identified correctly more often than the (untrained) face images that were not symmetrical to the trained view. If participants had correctly learned an image trained in phases 1 and 2, they should then be able to correctly recognise the same image at this final stage (e.g. when learned in 45° and tested in 45°). For this reason, only identities that were correctly recognised 100% of the time in the test stage when tested in the same viewpoint as they

were learned, were retained for analysis. The recognition of symmetric and non-symmetric responses was compared using a paired t-test. The recognition rate between different viewpoints was then used as a model in a regression analysis of the fMRI data in different regions.

RESULTS

Experiment 1

Figure 2 shows the results of the MVPA analysis demonstrating the similarity in the patterns of response to different viewpoint directions in the (A) face and (B) visual field regions. To determine whether there were distinct patterns of response to individual viewpoint directions, within-viewpoint (e.g. -90°, -90°) correlations were compared to between-viewpoint (e.g. -90°, -45°) correlations.

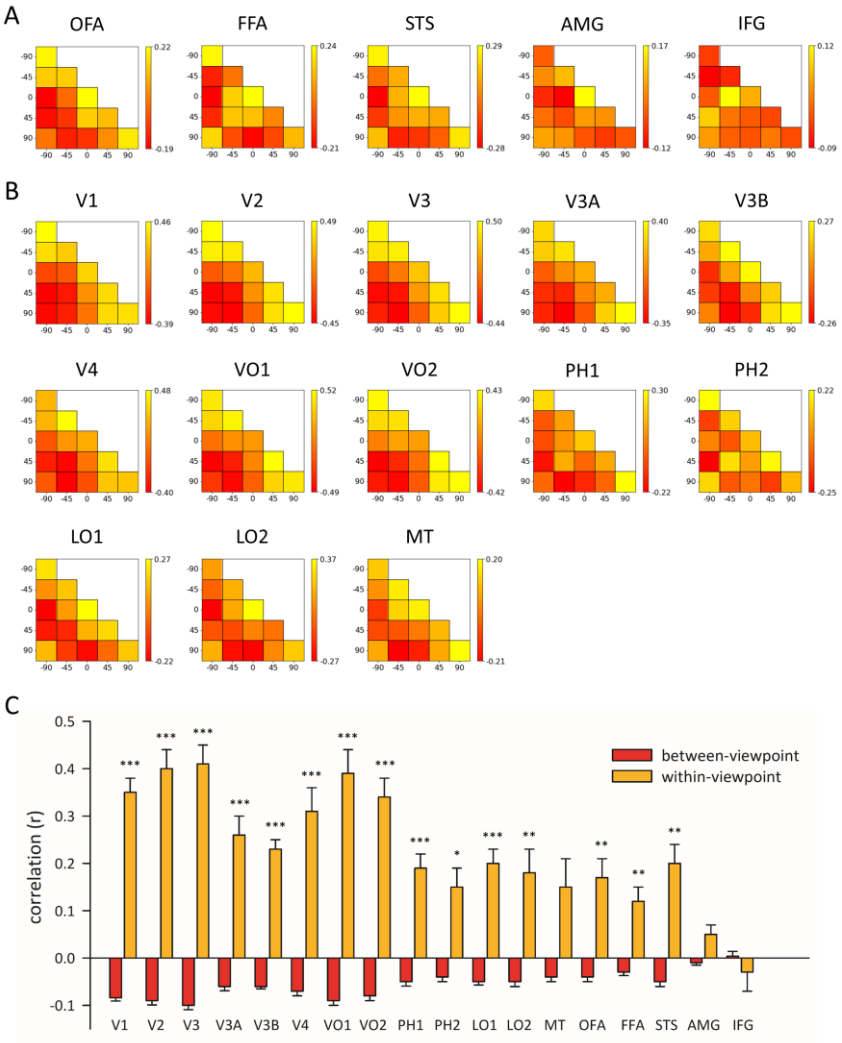

Figure 2 Correlation matrices showing the similarity in the patterns of response across viewpoints in (A) face-selective and (B) visual field regions. (C) Distinct patterns of response were demonstrated by higher within-viewpoint correlations compared to between-viewpoint correlations. *** $p < 0.001$, ** $p < 0.01$, * $p < 0.05$

There was a significant difference between within-viewpoint compared to between-viewpoint correlations in all face regions except the AMG and IFG (Fig. 2C and Table 1). To determine if the size of the face regions was important, we repeated the analysis with smaller (200 voxel) masks and found a similar pattern of results (Table 1-1). There was also significant difference between within-viewpoint compared to between-viewpoint correlations across many visual field areas. This overall pattern demonstrates that there are distinct representations of particular face viewpoints across visual cortex.

Table 1 Within-viewpoint and between-viewpoint correlations and associated paired t-tests across all ROIs. Further analysis is presented in the Extended Data Table 1-1 & Table 1-2.

	Correlation (r)			
ROI	Within-viewpoint	Between-viewpoint	t	$p_{corrected}$
V1	.35	-.08	10.07	<.001
V2	.40	-.10	9.33	<.001
V3	.41	-.10	9.98	<.001
V3A	.26	-.06	6.42	<.001
V3B	.23	-.06	10.35	<.001
V4	.31	-.08	5.90	<.001
VO1	.39	-.10	7.01	<.001
VO2	.34	-.08	7.74	<.001
PH1	.19	-.05	5.32	<.001
PH2	.15	-.04	3.52	.011
LO1	.20	-.05	6.77	<.001
LO2	.18	-.05	3.79	.007
MT	.15	-.04	2.46	*ns*
OFA	.17	-.04	4.47	.002
FFA	.12	-.03	3.89	.007
STS	.20	-.05	4.41	.002
AMG	.05	-.01	2.47	*ns*
IFG	-.03	.00	-0.60	*ns*

Next, we asked how similar the pattern of response to viewpoint was across all the ROIs by comparing the neural correlation matrices in Fig 2A and 2B. Figure 3A shows the

similarity in the representation of viewpoint across all regions. To determine the pattern of similarity in the representation across regions, a hierarchical clustering analysis was performed using an unweighted average distance method for computing the distance between clusters and the '1 minus correlation' values as the distance metric (Fig. 3B). The distinct clusters shown by the output of the clustering show that the way viewpoint is represented differs between regions.

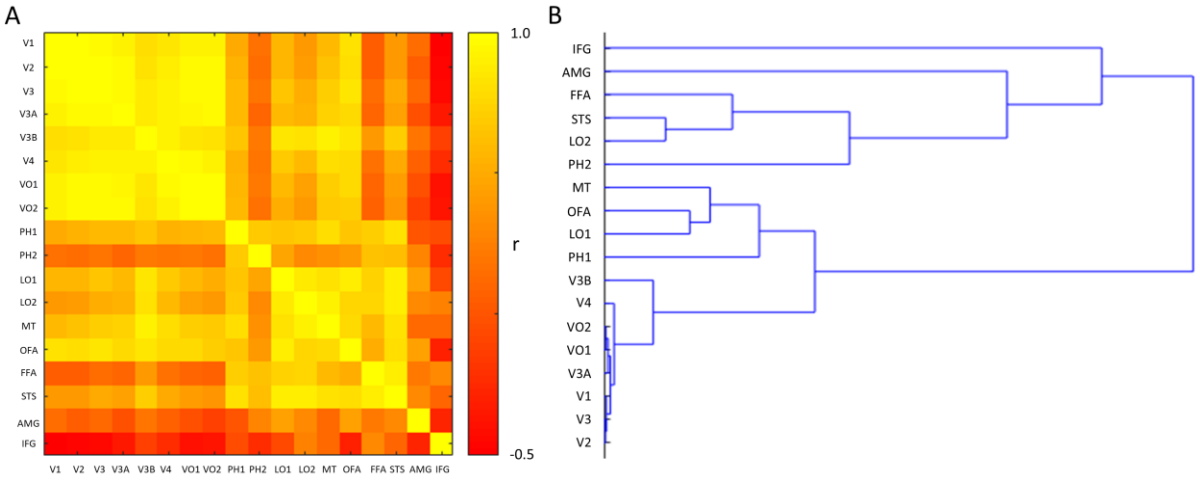

Figure 3 (A) Representational similarity matrix showing the similarity in the neural representations across regions. (B) Hierarchical clustering analysis showing regions with similar patterns of response to face viewpoint.

To determine how viewpoint is represented in different regions, our next analysis investigated how three different models of viewpoint representation were able to predict patterns of response. Figure 4 and Table 2 show the models for each representation and the corresponding regression coefficient for each region. To determine if the size of the face regions was important, we repeated the analysis with smaller (200 voxel) masks and found a similar pattern of results (Table 2-1). The analysis was also repeated across all regions with

multiple regression (Table 2-2) and using a permutation test for statistical significance (Table 2-3).

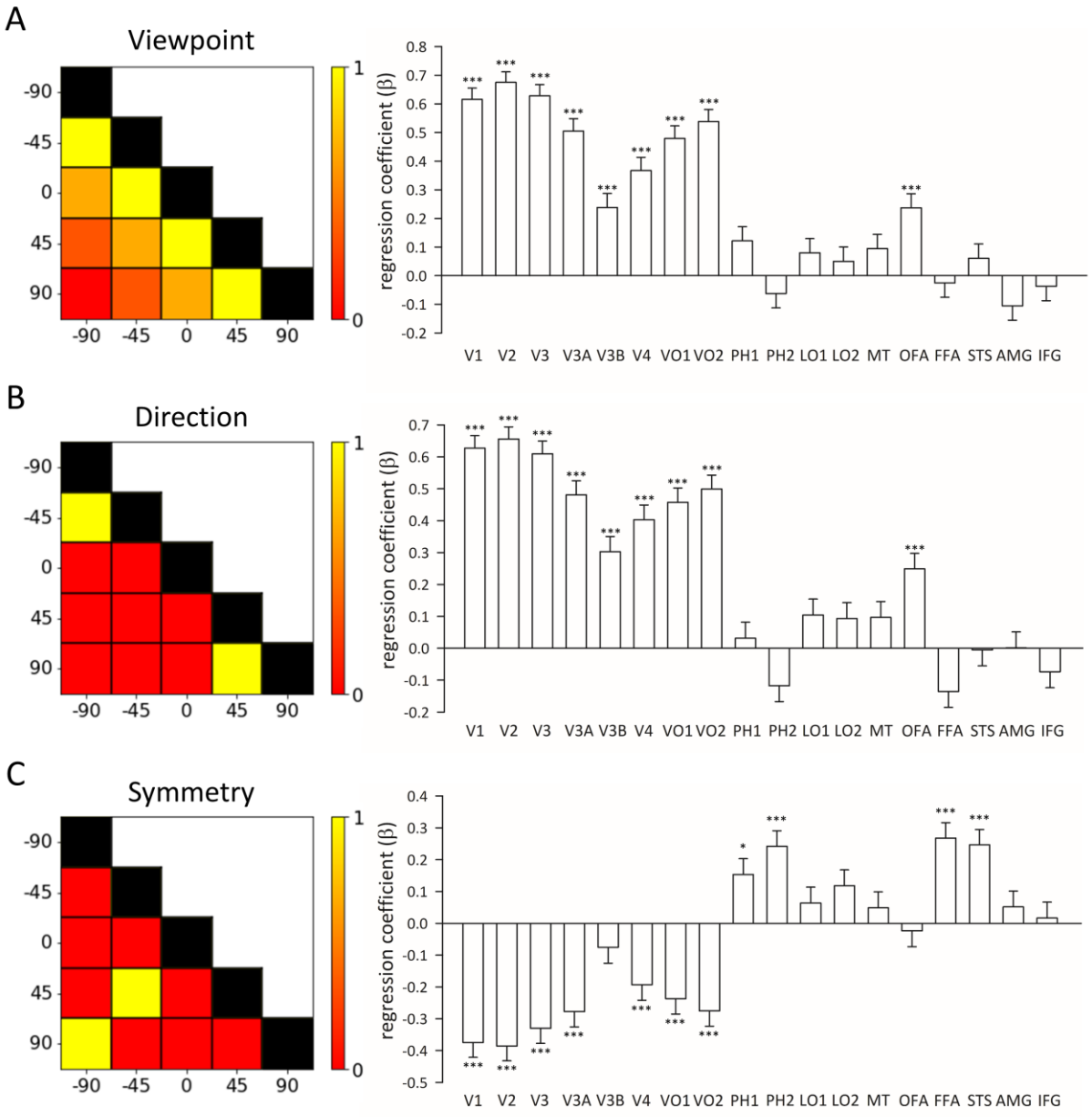

Figure 4 Regression analysis of fMRI data showing how different models predict patterns of response to viewpoint in different regions. (A) The Viewpoint and (B) Direction models predict the representational similarity in low-level visual areas. (C) In contrast, the symmetry model predicted patterns in high-level regions including the FFA and STS. *** $p < 0.001$, ** $p < 0.01$, * $p < 0.05$

Table 2 Regression coefficients for the viewpoint representation models across all ROIs. Further analysis is presented in the Extended Data Tables 2-1, 2-2 & 2-3.

	Viewpoint		Direction		Symmetry	
ROI	β	$p_{corrected}$	β	$p_{corrected}$	β	$p_{corrected}$
V1	.62	<.001	.63	<.001	-.37	<.001
V2	.67	<.001	.66	<.001	-.39	<.001
V3	.63	<.001	.61	<.001	-.33	<.001
V3A	.51	<.001	.48	<.001	-.28	<.001
V3B	.24	<.001	.30	<.001	-.08	*ns*
V4	.37	<.001	.40	<.001	-.19	.001
VO1	.48	<.001	.46	<.001	-.24	<.001
VO2	.54	<.001	.50	<.001	-.28	<.001
PH1	.12	*ns*	.03	*ns*	.15	.019
PH2	-.06	*ns*	-.12	*ns*	.24	<.001
LO1	.08	*ns*	.10	*ns*	.06	*ns*
LO2	.05	*ns*	.09	*ns*	.12	*ns*
MT	.09	*ns*	.10	*ns*	.05	*ns*
OFA	.24	<.001	.25	<.001	-.02	*ns*
FFA	-.03	*ns*	-.14	*ns*	.27	<.001
STS	.06	*ns*	-.01	*ns*	.25	<.001
AMG	-.11	*ns*	.00	*ns*	.05	*ns*
IFG	-.04	*ns*	-.07	*ns*	.02	*ns*

The Viewpoint and Direction models (Fig 4A/B) showed a similar pattern with high coefficients in the early visual field regions (V1-V4) and in some of the ventral temporal visual field regions (VO1-VO2). However, the coefficient values were not significant in the lateral occipital visual field regions (LO1, LO2) and the face-selective regions. The only exception was the OFA, which had a significant regression coefficient for both Viewpoint and Direction. The Symmetry model (Fig. 4C) showed an opposite pattern of results. We

found significant but negative coefficients in the early visual field regions (V1-V4) and in some of the ventral visual field regions (VO1-VO2). In contrast, there were significant positive coefficients in other ventral visual field regions (PH1-PH2) and in the FFA and STS. The OFA did not show a significant effect for symmetry. The AMG and IFG did not show significant coefficients for any of the three models.

We also analysed our data to ask whether low-level differences can account for the pattern of data. To investigate the effects of low-level image properties on patterns of neural response in face-selective regions, the image statistics of each object were computed using the GIST descriptor (Oliva & Torralba, 2001). For each image, a vector of 2048 values was obtained by passing the image through a series of 32 Gabor filters (eight orientations at four spatial frequencies), and windowing the filtered images along a 8 x 8 grid or 64 spatial locations. Each vector represents the image in terms of the output of each gabor filter at each position across the image (Rice et al., 2014; Watson et al., 2014; Watson et al., 2016). Image similarities between conditions were measured by correlating the GIST descriptors for all combinations of images. The similarity matrix of the correlation values for the GIST descriptor across all pairwise combinations of conditions was then used as a regressor in a regression analysis with the fMRI data. Table 3 shows that, consistent with previous studies (Rice et al., 2014; Watson et al., 2016; Weibert et al., 2018), low-level stimulus properties can account for some of the variance in the patterns of response in early visual field areas but also in higher visual areas such as the core face regions (OFA, FFA, STS).

Table 3 Regression coefficients for a model of low-level image properties across ROIs.

	GIST	
ROI	β	$p_{corrected}$
V1	.48	<.001
V2	.53	<.001
V3	.51	<.001
V3A	.40	<.001
V3B	.24	<.001
V4	.30	<.001
VO1	.39	<.001
VO2	.43	<.001
PH1	.19	.001
PH2	.04	*ns*
LO1	.17	.004
LO2	.15	.017
MT	.13	.028
OFA	.27	<.001
FFA	.15	.012
STS	.22	<.001
AMG	-.09	*ns*
IFG	-.01	*ns*

Experiment 2

Experiment 2 aimed to assess the perceptual experience of facial viewpoint symmetry. Participants were presented with pairs of faces which showed different viewpoints and were asked to rate how similar they believed the images were on a scale of 1 to 7 (1: less similar, 7: more similar). A similarity matrix of each of the viewpoint combinations can be seen in Figure 5A. In order to assess whether participants rate symmetrical directions more similar than non-symmetrical directions, data were averaged across symmetrical and non-

symmetrical pairings. Participants rated symmetrical viewpoints as more similar than non-symmetrical viewpoint conditions ($t(19) = 6.37$, $p < .001$).

Next, we asked whether the pattern of response in the perceptual similarity task could predict the patterns of response in different regions of the brain (Fig. 5A, right). Using a regression analysis with perceptual similarity as the model, we found that responses from V1 were not predicted by the pattern of perceptual similarity. However, the correlation coefficients showed a progressive increase along the visual hierarchy with the highest regression coefficients in the FFA and STS (Table 3). This shows a clear link between the perceptual similarity of different viewpoints and the pattern of response in some face regions.

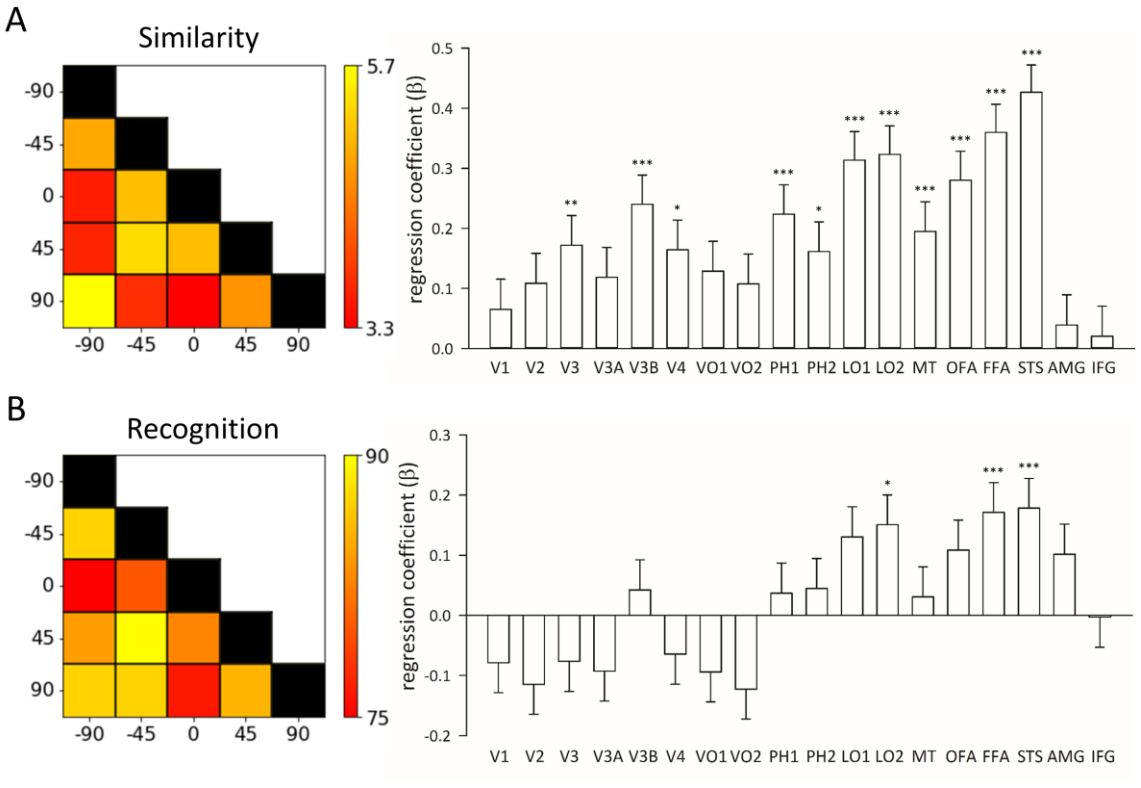

Figure 5 (A) Perceptual similarity ratings between viewpoint directions (left). A regression analysis using the perceptual similarity ratings as a model showed an increase in the coefficients from low-level to high-level visual regions, with the highest values in the FFA and STS. (B) Recognition rates for

different combinations of viewpoint during the training and test phases of the recognition experiment (left). A regression analysis using the recognition values as a model showed an increase in the coefficients from low-level to high-level regions, with the highest values in the FFA and STS. *** $p < 0.001$, ** $p < 0.01$, * $p < 0.05$

Experiment 3

The aim of Experiment 3 was to determine if learning a face at a particular viewpoint conferred an advantage in the recognition of the symmetric viewpoint. Figure 5B shows the % recognition rates for different combinations of viewpoint from training and test phases of the experiment. In order to compare performance across symmetrical and non-symmetrical conditions, data were averaged across symmetrical and non-symmetrical viewpoint combinations. Participants performed significantly better when tested with a viewpoint that was symmetrical to the one which they had learned ($t(47)= 2.63$, $p = .012$).

Next, we asked whether accuracy in the recognition task could predict the patterns of response in different regions of the brain (Fig. 5B, right). Using a regression analysis with recognition accuracy as the model, we found that early visual areas were not significant. In contrast, only LO2, FFA and STS showed positive regression coefficients (Table 3). This demonstrates a link between behavioural performance on a face learning task and patterns of response in the face-selective regions, such as the FFA.

To determine if the size of the face regions was important, we repeated the analysis of Experiment 2 and Experiment 3 with smaller (200 voxel) masks and found a similar pattern of results (Table 4-1). The analysis was also repeated across all regions with multiple regression (Table 4-2). A multiple regression found significant effects of Similarity across many visual areas, but was largest in the FFA and STS. However, we did not find any

418 additional benefit of the Recognition model. This is likely explained by the similarity in the
419 models which have a correlation of r = 0.53. Finally, we reanalysed the data using a
420 permutation test for statistical significance (Table 4-3).

421
422 **Table 4** Regression coefficients demonstrating the ability of the behavioural data from Exp 2
423 (Similarity ratings) and Exp 3 (Recognition) in predicting the neural responses across all ROIs. Further
424 analysis is presented in the Extended Data Tables 4-1, 4-2 & 4-3.

	Similarity		Recognition	
ROI	β	$p_{corrected}$	β	$p_{corrected}$
V1	.07	*ns*	-.08	*ns*
V2	.11	*ns*	-.11	*ns*
V3	.17	.006	-.08	*ns*
V3A	.12	*ns*	-.09	*ns*
V3B	.24	<.001	.04	*ns*
V4	.16	.010	-.06	*ns*
VO1	.13	*ns*	-.09	*ns*
VO2	.11	*ns*	-.12	*ns*
PH1	.22	<.001	.04	*ns*
PH2	.16	.011	.05	*ns*
LO1	.31	<.001	.13	*ns*
LO2	.32	<.001	.15	.043
MT	.20	.001	.03	*ns*
OFA	.28	<.001	.11	*ns*
FFA	.36	<.001	.17	.011
STS	.43	<.001	.18	.006
AMG	.04	*ns*	.10	*ns*
IFG	.02	*ns*	-.00	*ns*

425

426

DISCUSSION

The aim of this study was to investigate and understand responses to symmetric views of real human faces in face-selective regions of the human brain. A viewpoint-symmetric representation was found in the FFA and STS, but not in the OFA (Experiment 1). To determine whether a symmetrical representation of viewpoint can convey an advantage in the perception and recognition of faces, participants performed a perceptual similarity and a face recognition task. We found that symmetric viewpoints were perceived to be more similar than non-symmetric viewpoints (Experiment 2) and that identities learnt at a particular viewpoint were more accurately recognized at the symmetrical viewpoint compared to non-symmetrical viewpoints (Experiment 3). Critically, these behavioural judgements of symmetry and recognition across different views were able to predict patterns of response in face-selective brain regions.

Previous neurophysiological studies have found a large number of neurons with maximal responses to specific viewpoints (Dubois et al., 2015; Freiwald & Tsao, 2010; Perrett et al., 1998, 1991). We also found distinct patterns of response to viewpoint throughout visual cortex. Our findings are therefore consistent with previous neuroimaging studies that have also found distinct patterns of response to specific viewpoints (Axelrod & Yovel, 2012; Carlin et al., 2011; Dubois et al., 2015; Guntupalli et al., 2017; Kietzmann et al., 2012; Ramirez et al., 2014). These neural responses to viewpoint are also consistent with behavioural studies that have shown the importance of viewpoint-selective representations in the perception and recognition of unfamiliar faces (Bruce, 1982; Fang & He, 2005; Hill & Bruce, 1996; Longmore et al., 2008).

This widespread evidence of viewpoint selectivity to face images across the visual cortex provides a challenge to understanding how invariant representations of facial identity are achieved (Perrett et al., 1998). One possibility is that different viewpoint-selective units converge to generate invariant units of facial identity, similar to the face recognition units suggested by cognitive models of face recognition (Bruce & Young, 1986; Burton et al., 1999). However, the discovery of neurons that are tuned to symmetric viewpoints of the face has led to the idea that these may provide an important intermediate computational step before full invariance is achieved (Freiwald & Tsao, 2010), or at least facilitate the process. Evidence that these viewpoint symmetric representations are found in the human brain comes from neuroimaging studies, which have found that the patterns of response in face regions to symmetrical viewpoints are more similar than to non-symmetrical viewpoints (Axelrod & Yovel, 2012; Guntupalli et al., 2017; Kietzmann et al., 2012, 2017). However, there has been some inconsistency in the literature about which regions show a symmetrical representation of faces. Kietzmann and colleagues found viewpoint symmetry represented in the OFA and FFA. However, other studies report symmetrical representations in the FFA and STS, but not in the OFA, leading them to conclude that there is a hierarchical processing of face viewpoint in face regions (Axelrod & Yovel, 2012; Guntupalli et al., 2017). Finally, Ramirez and colleagues (Ramírez, 2018; Ramírez, 2017; Ramirez et al., 2014) have argued that symmetry responses in the FFA could be better explained by a view-dependent mechanism. In contrast, to the current and previous studies, they presented faces in the periphery to test the invariance of viewpoint symmetry. So, it is possible that a lack of position invariance could explain the difference in results across studies (see Kietzmann et al., 2017). Another possible reason for the difference in results could be the methodological choices in MVPA. However, view symmetry in faces has

been shown across different studies that have used a range of MVPA approaches (Axelrod & Yovel, 2012; Guntupalli et al., 2017; Kietzmann et al., 2012, 2017).

To determine where viewpoint symmetry is represented, we compared how three different models (Viewpoint, Direction and Symmetry) predicted patterns of neural response in different regions of visual cortex. The predictions of the Viewpoint model were exclusively based on the angular separation between the different viewpoints, the Direction model coded whether combinations of viewpoints were both left-facing or right-facing, and the Symmetry model explicitly allowed different symmetric orientations (e.g. -45 and +45, or -90 and +90) to be represented as similar to each other regardless of the angular separations themselves (which are 180 degrees for -90 and +90 images and only 90 degrees for -45 and +45 images).

We found that the Viewpoint and Direction models best predicted responses in early visual cortex (V1-V4) and the OFA, but showed a gradual decline in high-level regions and were not able to explain the patterns in the FFA and STS. In contrast, the patterns of response in the FFA and STS (but not the OFA) were best predicted by the Symmetry model. These findings are consistent with a hierarchical organization of viewpoint responsiveness across visual regions in which more posterior regions have view-dependent representations, but more anterior regions (including classic face-selective regions) are sensitive to viewpoint symmetry (Axelrod & Yovel, 2012; Freiwald & Tsao, 2010; Guntupalli et al., 2017; Kietzmann et al., 2012, 2017).

Although our results provide further support for the representation of viewpoint symmetry in face-selective neural regions, such as the FFA, it has not been clear whether these representations are important for the perception and recognition of faces. That is, the

link between neural and behavioural measures has not been investigated directly. To address this issue, we compared symmetrical and non-symmetrical views in a perceptual similarity task and a recognition task. We found that symmetrical views of the face are perceived to be more similar than non-symmetrical views. Similarly, we found that novel face images that were symmetric to a learned face view were recognized better than non-symmetric face views. These results are consistent with previous studies that have shown a behavioural advantage for symmetric compared to non-symmetric viewpoints (Busey & Zaki, 2004; Troje & Bülthoff, 1998). However, to investigate the link between symmetric and non-symmetric viewpoints and neural responses, we used the data from our behavioural results to predict patterns of response across visual cortex. The data from both the perceptual similarity and recognition experiments showed a progressive increase in their ability to predict neural responses from low-level to high-level regions. Patterns of response in face regions such as the FFA and STS were predicted best by performance on both the perceptual similarity and recognition tasks. This provides the first evidence for a close link between symmetrical representations in the brain and a behavioural advantage in the recognition of faces.

A crucial difference between this study and many previous studies investigating symmetry is the use of real faces. Many previous studies have used computer generated faces that are often themselves mirror symmetric. However, human faces are not actually completely symmetrical (see Figure 1). So, if the brain uses symmetry in order to assist reaching viewpoint invariance, it needs to be able to allow for these deviations from symmetry found in real human faces. We have been able to show that neural and behavioural responses are able to compensate for this lack of full mirror symmetry.

519 Although this study has focussed on face processing, a preference for bilateral
520 symmetry is a more general property of the visual system (Bertamini et al., 2018; Keefe et
521 al., 2018). The bias in neural processing is also evident in perceptual judgements showing
522 that we are adept at discriminating small deviations in bilateral symmetry (Corballis & Beale,
523 1976; Rhodes et al., 2005) and find bilaterally symmetrical images more aesthetically
524 pleasing than non-symmetric images (Jacobsen et al., 2006; Makin et al., 2012). Our study
525 differs from these studies as bilateral symmetry is not evident in any one image itself.
526 Rather, we have shown that symmetry enhances the integration over time of two images.
527 Nevertheless, we did find that sensitivity to viewpoint symmetry was evident in regions such
528 as PH1 and PH2. Future studies will be necessary to determine the extent to which similar
529 neural and perceptual mechanisms are involved in both processes.

530 An important feature of our findings is that the spatial patterns of response to
531 viewpoint generalized across participants. This observation complements other
532 neuroimaging studies using univariate methods that have already shown that the locations
533 of face-selective regions in the ventral visual pathway are broadly consistent across
534 individuals (Davies-Thompson & Andrews, 2012; Kanwisher et al., 1997). This implies that
535 common principles may well underpin the organization of these regions. In our analysis, we
536 used multivariate methods to compare the spatial pattern of response in each individual
537 with the spatial pattern from the rest of the group of participants (Coggan et al., 2016;
538 Poldrack et al., 2009; Rice et al., 2014; Watson et al., 2014; Weibert et al., 2018). The
539 success of this approach implies that much of the topographic pattern of response to facial
540 viewpoint is consistent across individuals. Of course, it is possible that a finer-grained
541 within-participant analysis could reveal more information. However, it is unclear how this

could lead to a completely different pattern of response. Indeed, our results are consistent with many previous studies using within-participant analyses (Axelrod & Yovel, 2012; Guntupalli et al., 2017; Kietzmann et al., 2012). These observations are significant in that they suggest that our findings reflect the operation of large-scale organizing principles that are consistent across different individuals.

In conclusion, our results demonstrate that the spatial patterns of responses to facial viewpoint in the FFA and STS are sensitive to symmetry. A model that explicitly represented image symmetry was better able to predict patterns of response in these face regions than models based exclusively on image viewpoint or direction. We also found that symmetrical viewpoints are perceived to be more similar and are more easily recognized than non-symmetrical viewpoints in purely behavioural tasks. Finally, we were able to establish a direct link between the neuroimaging and behavioural findings by showing that these behavioural data could predict patterns of response in face-selective regions, such as the FFA and STS. Together, these results support the idea that symmetrical representations are an important computational step in the generation of view-invariant representations of faces that are essential to familiar face recognition.

561 **REFERENCES**

562

563 Andrews, T. J., & Ewbank, M. P. (2004). Distinct representations for facial identity and changeable
564 aspects of faces in the human temporal lobe. *NeuroImage*, *23*(3), 905–913.

565 Axelrod, V., & Yovel, G. (2012). Hierarchical processing of face viewpoint in human visual cortex.
566 *Journal of Neuroscience*, *32*(7), 2442–2452.

567 Bruce, V. (1982). Changing faces: visual and non-visual coding processes in face recognition. *British*
568 *Journal of Psychology, 73*, 105-116.

569 Bruce, V., & Young, A. W. (1986). Understanding face recognition. *British Journal of Psychology*, *77*,
570 305–327.

571 Burton, A. M., Bruce, V., & Hancock, P. J. B. (1999). From pixels to people: A model of familar face
572 recognition. *Cognitive Science*, *23*(1), 1–31.

573 Busey, T. A., & Zaki, S. R. (2004). The contribution of symmetry and motion to the recognition of
574 faces at novel orientations. *Memory and Cognition*, *32*(6), 916–931.

575 Carlin, J. D., Calder, A. J., Kriegeskorte, N., Nili, H., & Rowe, J. B. (2011). A Head View-Invariant
576 Representation of Gaze Direction in Anterior Superior Temporal Sulcus. *Current Biology*, *21*(21),
577 1817–1821.

578 Coggan, D. D., Liu, W., Baker, D. H., & Andrews, T. J. (2016). Category-selective patterns of neural
579 response in the ventral visual pathway in the absence of categorical information. *NeuroImage*,
580 *135*, 107–114.

581 Corballis, M. C., & Beale, I. L. (1976). *The psychology of left and right.* Oxford, England: Lawrence
582 Erlbaum.

583 Davies-Thompson, J., & Andrews, T. J. (2012). Intra- and Inter-Hemispheric Connectivity Between
584 Face-Selective Regions in the Human Brain. *Journal of Neurophysiology*, *108*, 3087–3095.

585 Dubois, J., de Berker, A. O., & Tsao, D. Y. (2015). Single-unit recordings in the macaque face patch

system reveal limitations of fMRI MVPA. *Journal of Neuroscience*, *35*(6), 2791–2802.

Eger, E., Schweinberger, S. R., Dolan, R. J., & Henson, R. N. (2005). Familiarity enhances invariance of face representations in human ventral visual cortex: fMRI evidence. *NeuroImage*, *26*(4), 1128–1139.

Ewbank, M. P., & Andrews, T. J. (2008). Differential sensitivity for viewpoint between familiar and unfamiliar faces in human visual cortex. *NeuroImage*, *40*(4), 1857–1870.

Fang, F., & He, S. (2005). Viewer-centered object representation in the human visual system revealed by viewpoint aftereffects. *Neuron*, *45*(5), 793–800.

Fang, F., Murray, S. O., & He, S. (2007). Duration-dependent fMRI adaptation and distributed viewer-centered face representation in human visual cortex. *Cerebral Cortex*, *17*(6), 1402–1411.

Freiwald, W. A., & Tsao, D. Y. (2010). Functional compartmentalization and viewpoint generalization within the macaque face-processing system. *Science*, *330*(6005), 845–851.

Grill-Spector, K., Kushnir, T., Edelman, S., Avidan, G., Itzchak, Y., & Malach, R. (1999). Differential processing of objects under various viewing conditions in the human lateral occipital complex. *Neuron*, *24*(1), 187–203.

Guntupalli, J. S., Wheeler, K. G., & Gobbini, M. I. (2017). Disentangling the Representation of Identity from Head View Along the Human Face Processing Pathway. *Cerebral Cortex*, *27*(1), 46–53.

Hancock, P. J. B., Bruce, V., & Burton, A. M. (2000). Recognition of unfamiliar faces. *Trends in Cognitive Sciences*, *4*(9), 330–337.

Hanke, M., Halchenko, Y. O., Sederberg, P. B., Hanson, S. J., Haxby, J. V, & Pollmann, S. (2009). PyMVPA: A python toolbox for multivariate pattern analysis of fMRI data. *Neuroinformatics*, *7*(1), 37–53.

Haxby, J. V, Gobbini, M. I., Furey, M. L., Ishai, A., Schouten, J. L., & Pietrini, P. (2001). Distributed and overlapping representations of faces and objects in ventral temporal cortex. *Science*,

610 *293*(5539), 2425–2430.

611 Hill, H., & Bruce, V. (1996). Effects of Lighting on the Perception of Facial Surfaces. *Journal of*
612 *Experimental Psychology: Human Perception and Performance*, *22*(4), 986–1004.

613 Jacobsen, T., Schubotz, R. I., Höfel, L., & Cramon, D. Y. V. (2006). Brain correlates of aesthetic
614 judgment of beauty. *NeuroImage*, *29*(1), 276–285.

615 Kanwisher, N., McDermott, J., & Chun, M. M. (1997). The fusiform face area: a module in human
616 extrastriate cortex specialized for face perception. *Journal of Neuroscience*, *17*(11), 4302–4311.

617 Kietzmann, T. C., Gert, A., & König, P. (2015). Representational dynamics of facial viewpoint
618 encoding: Head orientation, viewpoint symmetry, and front-on views. *Journal of Vision*, *15*(12),
619 750.

620 Kietzmann, T. C., Gert, A. L., Tong, F., & Konig, P. (2017). Reperesentational Dynamics of Facial
621 Viewpoint Encoding. *Journal of Cognitive Neuroscience*, *29*(4), 637–651.

622 Kietzmann, T. C., Swisher, J. D., Konig, P., & Tong, F. (2012). Prevalence of Selectivity for Mirror-
623 Symmetric Views of Faces in the Ventral and Dorsal Visual Pathways. *Journal of Neuroscience*,
624 *32*(34), 11763–11772.

625 Kriegeskorte, N., Mur, M., & Bandettini, P. A. (2008). Representational similarity analysis-connecting
626 the branches of systems neuroscience. Frontiers in Systems Neuroscience, 2: 4.

627 Langner, O., Dotsch, R., Bijlstra, G., Wigboldus, D. H. J., Hawk, S. T., & van Knippenberg, A. (2010).
628 Presentation and validation of the Radboud Faces Database. *Cognition & Emotion*, *24*(8), 1377–
629 1388.

630 Longmore, C. A., Liu, C. H., & Young, A. W. (2008). Learning faces from photographs. *Journal of*
631 *Experimental Psychology. Human Perception and Performance*, *34*(1), 77–100.

632 Makin, A. D. J., Pecchinenda, A., & Bertamini, M. (2012). Implicit affective evaluation of visual
633 symmetry. *Emotion*, *12*(5), 1021–1030.

Perrett, D. I., Oram, M. W., & Ashbridge, E. (1998). Evidence accumulation in cell populations responsive to faces: An account of generalisation of recognition without mental transformations. *Cognition*, *67*(1–2), 111–145.

Perrett, D. I., Oram, M. W., Harries, M. H., Bevan, R., Hietanen, J. K., Benson, P. J., & Thomas, S. (1991). Viewer-centred and object-centred coding of heads in the macaque temporal cortex. *Experimental Brain Research*, *86*(1), 159–173.

Poldrack, R. A., Halchenko, Y. O., & Hanson, S. J. (2009). Decoding the large-scale structure of brain function by classifying mental States across individuals. *Psychological Science*, *20*(11), 1364–1372.

Pourtois, G., Schwartz, S., Seghier, M. L., Lazeyras, F., & Vuilleumier, P. (2005). View-independent coding of face identity in frontal and temporal cortices is modulated by familiarity: An event-related fMRI study. *NeuroImage*, *24*(4), 1214–1224.

Ramírez, F. M. (2018). Orientation Encoding and Viewpoint Invariance in Face Recognition: Inferring Neural Properties from Large-Scale Signals. *The Neuroscientist : A Review Journal Bringing Neurobiology, Neurology and Psychiatry*, 1073858418769554.

Ramirez, F. M., Cichy, R. M., Allefeld, C., & Haynes, J.-D. (2014). The Neural Code for Face Orientation in the Human Fusiform Face Area. *Journal of Neuroscience*, *34*(36), 12155–12167.

Rhodes, G., Peters, M., Lee, K., Morrone, M. C., & Burr, D. (2005). Higher-level mechanisms detect facial symmetry. *Proceedings. Biological Sciences / The Royal Society*, *272*(1570), 1379–1384.

Rice, G. E., Watson, D. M., Hartley, T., & Andrews, T. J. (2014). Low-Level Image Properties of Visual Objects Predict Patterns of Neural Response across Category-Selective Regions of the Ventral Visual Pathway. *Journal of Neuroscience*, *34*(26), 8837–8844.

Sormaz, M., Watson, D. M., Smith, W. A. P., Young, A. W., & Andrews, T. J. (2016). Modelling the perceptual similarity of facial expressions from image statistics and neural responses.

NeuroImage, *129*, 64–71.

Sutherland, C. A. M., Young, A. W., & Rhodes, G. (2017). Facial first impressions from another angle: how social judgments are influenced by changeable and invariant facial properties. *British Journal of Psychology, 108*, 397-415.

Troje, N. F., & Bülthoff, H. H. (1998). How is bilateral symmetry of human faces used for recognition of novel views? *Vision Research*, *38*(1), 79–89.

Wang, L., Mruczek, R. E. B., Arcaro, M. J., & Kastner, S. (2015). Probabilistic maps of visual topography in human cortex. *Cerebral Cortex*, *25*(10), 3911–3931.

Watson, D. M., Hartley, T., & Andrews, T. J. (2014). Patterns of response to visual scenes are linked to the low-level properties of the image. *NeuroImage*, *99*, 402–410.

Weibert, K., Flack, T. R., Young, A. W., & Andrews, T. J. (2018). Patterns of neural response in face regions are predicted by low-level image properties. *Cortex*, *103*, 199–210.

Young, A. W. (2018). Faces, people and the brain: the 45th Sir Frederic Bartlett Lecture. *Quarterly Journal of Experimental Psychology, 71,* 569-594.

Young, A. W., & Burton, A. M. (2017). Recognizing faces. *Current Directions in Psychological Science, 26*, 212-217.

Table 1-1 Within-viewpoint and between-viewpoint correlations and associated paired t-tests across all face regions defined with 200 voxel masks.

	Correlation (r)			
ROI	Within-viewpoint	Between-viewpoint	t	$P_{corrected}$
OFA	.16	-.04	3.50	.007
FFA	.15	-.03	4.11	.003
STS	.20	-.05	3.70	.006
AMG	.07	-.02	3.32	.007
IFG	.01	.00	0.24	*ns*

Table 2-1 Regression coefficients for the viewpoint representation models across all face regions defined with 200 voxel masks.

	Viewpoint		Direction		Symmetry	
ROI	β	$p_{corrected}$	β	$p_{corrected}$	β	$p_{corrected}$
OFA	.18	.002	.25	<.001	-.05	*ns*
FFA	-.02	ns	-.15	.008	.28	<.001
STS	.14	.021	.07	*ns*	.13	.037
AMG	-.12	ns	.00	*ns*	.08	*ns*
IFG	-.02	ns	-.08	*ns*	.06	*ns*

Table 4-1 Regression coefficients demonstrating the ability of the behavioural data from Exp 2 (Similarity ratings) and Exp 3 (Recognition) in predicting the neural responses across all face regions defined with 200 voxel masks.

	Similarity		Recognition	
ROI	β	$p_{corrected}$	β	$p_{corrected}$
OFA	.20	<.001	.12	*ns*
FFA	.37	<.001	.16	.007
STS	.34	<.001	.08	*ns*
AMG	.06	*ns*	.10	*ns*
IFG	.04	*ns*	-.01	*ns*

686 **Table 2-2** Regression coefficients for the viewpoint representation models using multiple regression
687 across all ROIs.

	Viewpoint		Direction		Symmetry	
ROI	β	$p_{corrected}$	β	$p_{corrected}$	β	$p_{corrected}$
V1	.36	<.001	.43	<.001	-.09	*ns*
V2	.43	<.001	.43	<.001	-.07	*ns*
V3	.42	<.001	.39	<.001	-.02	*ns*
V3A	.34	<.001	.30	<.001	-.03	*ns*
V3B	.15	*ns*	.24	<.001	.06	*ns*
V4	.21	.002	.29	<.001	-.01	*ns*
VO1	.34	<.001	.29	<.001	.00	*ns*
VO2	.38	<.001	.31	<.001	-.01	*ns*
PH1	.28	<.001	-.04	*ns*	.28	<.001
PH2	.13	.032	-.11	*ns*	.28	<.001
LO1	.10	*ns*	.09	*ns*	.14	*ns*
LO2	.10	*ns*	.09	*ns*	.19	*ns*
MT	.13	*ns*	.07	*ns*	.13	*ns*
OFA	.21	.005	.17	.018	.13	*ns*
FFA	.22	.003	-.16	.029	.34	<.001
STS	.27	<.001	-.05	*ns*	.37	<.001
AMG	-.14	*ns*	.07	*ns*	.00	*ns*
IFG	.00	*ns*	-.07	*ns*	.00	*ns*

688
689

690 **Table 4-2** Regression coefficients demonstrating the ability of the behavioural data from Exp 2
691 (Similarity ratings) and Exp 3 (Recognition) in predicting the neural responses using multiple
692 regression across all ROIs.

	Similarity		Recognition	
ROI	β	*p*	β	*p*
V1	.15	.035	-.16	*ns*
V2	.23	<.001	-.24	<.001
V3	.29	<.001	-.23	<.001
V3A	.23	<.001	-.21	.003
V3B	.30	<.001	-.12	*ns*
V4	.27	<.001	-.21	.004
VO1	.25	<.001	-.22	.002
VO2	.24	<.001	-.25	<.001
PH1	.28	<.001	-.11	*ns*
PH2	.19	.005	-.06	*ns*
LO1	.34	<.001	-.05	*ns*
LO2	.34	<.001	-.03	*ns*
MT	.25	<.001	-.10	*ns*
OFA	.31	<.001	-.05	*ns*
FFA	.37	<.001	-.03	*ns*
STS	.46	<.001	-.06	*ns*
AMG	-.02	*ns*	.11	*ns*
IFG	.03	*ns*	-.02	*ns*

693
694
695

Table 2-3 Permutation analysis for the viewpoint representation models' ability to predict neural responses across ROIs. Permutation p-values have been corrected for multiple comparisons using the Bonferroni-Holm correction across ROIs. Critical values represent the 95th percentile of absolute permuted null distribution.

	Viewpoint			Direction			Symmetry		
ROI	β	Permutation $p_{corrected}$	Permutation critical value	β	Permutation $p_{corrected}$	Permutation critical value	β	Permutation $p_{corrected}$	Permutation critical value
V1	.62	<.001	0.099	.63	<.001	0.097	-.37	<.001	0.098
V2	.67	<.001	0.099	.66	<.001	0.098	-.39	<.001	0.099
V3	.63	<.001	0.099	.61	<.001	0.098	-.33	<.001	0.099
V3A	.51	<.001	0.098	.48	<.001	0.099	-.28	<.001	0.098
V3B	.24	<.001	0.098	.30	<.001	0.098	-.08	*ns*	0.099
V4	.37	<.001	0.097	.40	<.001	0.098	-.19	<.001	0.098
VO1	.48	<.001	0.098	.46	<.001	0.099	-.24	<.001	0.096
VO2	.54	<.001	0.098	.50	<.001	0.098	-.28	<.001	0.098
PH1	.12	*ns*	0.099	.03	*ns*	0.099	.15	.010	0.097
PH2	-.06	*ns*	0.096	-.12	*ns*	0.098	.24	<.001	0.098
LO1	.08	*ns*	0.097	.10	*ns*	0.097	.06	*ns*	0.099
LO2	.05	*ns*	0.097	.09	*ns*	0.097	.12	*ns*	0.099
MT	.09	*ns*	0.099	.10	*ns*	0.098	.05	*ns*	0.099
OFA	.24	<.001	0.099	.25	<.001	0.098	-.02	*ns*	0.099
FFA	-.03	*ns*	0.097	-.14	*ns*	0.097	.27	<.001	0.100
STS	.06	*ns*	0.099	-.01	*ns*	0.098	.25	<.001	0.100
AMG	-.11	*ns*	0.098	.00	*ns*	0.097	.05	*ns*	0.098
IFG	-.04	*ns*	0.101	-.07	*ns*	0.098	.02	*ns*	0.097

Table 4-3 Permutation analysis for simple linear regression demonstrating the ability of the behavioural data from Exp 2 and 3 in predicting the neural responses across all ROIs. Permutation p-values have been corrected for multiple comparisons using the Bonferroni-Holm correction across ROIs. Critical values represent the 95th percentile of absolute permuted null distribution.

	Similarity			Recognition		
ROI	β	Permutation $p_{corrected}$	Permutation critical value	β	Permutation $p_{corrected}$	Permutation critical value
V1	.07	*ns*	0.099	-.08	*ns*	0.098
V2	.11	*ns*	0.098	-.11	*ns*	0.097
V3	.17	.0030	0.099	-.08	*ns*	0.099
V3A	.12	*ns*	0.098	-.09	*ns*	0.099
V3B	.24	<.001	0.099	.04	*ns*	0.098
V4	.16	.009	0.098	-.06	*ns*	0.097
VO1	.13	*ns*	0.099	-.09	*ns*	0.010
VO2	.11	*ns*	0.098	-.12	*ns*	0.099
PH1	.22	<.001	0.099	.04	*ns*	0.099
PH2	.16	.013	0.098	.05	*ns*	0.099
LO1	.31	<.001	0.098	.13	*ns*	0.099
LO2	.32	<.001	0.098	.15	.045	0.099
MT	.20	.001	0.098	.03	*ns*	0.098
OFA	.28	<.001	0.099	.11	*ns*	0.096
FFA	.36	<.001	0.099	.17	.009	0.099
STS	.43	<.001	0.099	.18	.007	0.098
AMG	.04	*ns*	0.098	.10	*ns*	0.096
IFG	.02	*ns*	0.099	.00	*ns*	0.098

706

707

708 **Table 1-2** Total number of voxels for each region of interest. Voxel size = 2 x 2 x 2 mm.

ROI	Voxel Count
V1	1604
V2	1372
V3	1044
V3A	554
V3B	263
V4	328
VO1	153
VO2	253
PH1	175
PH2	165
LO1	324
LO2	125
MT	86

709

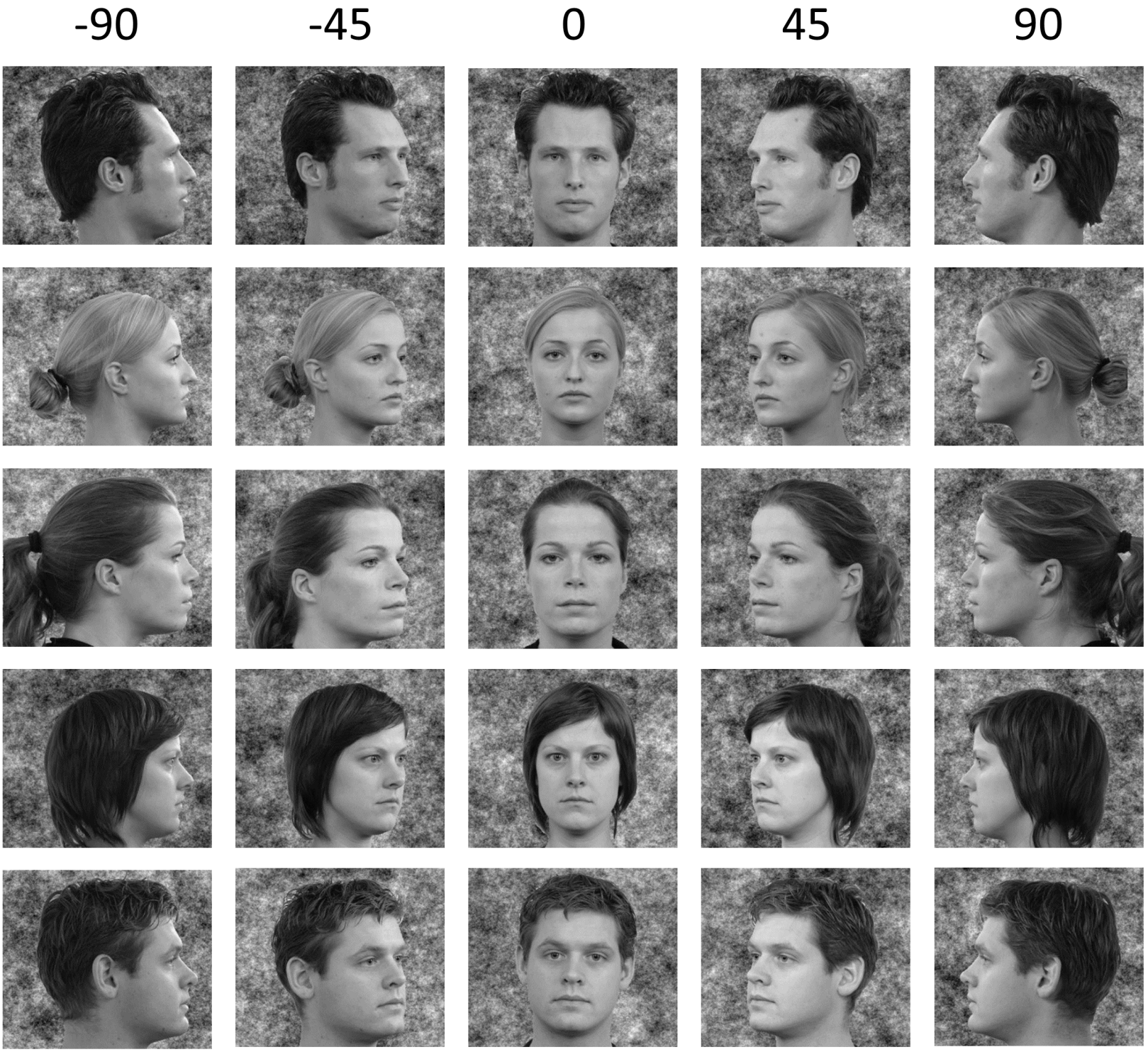
-90
-45
0
45
90

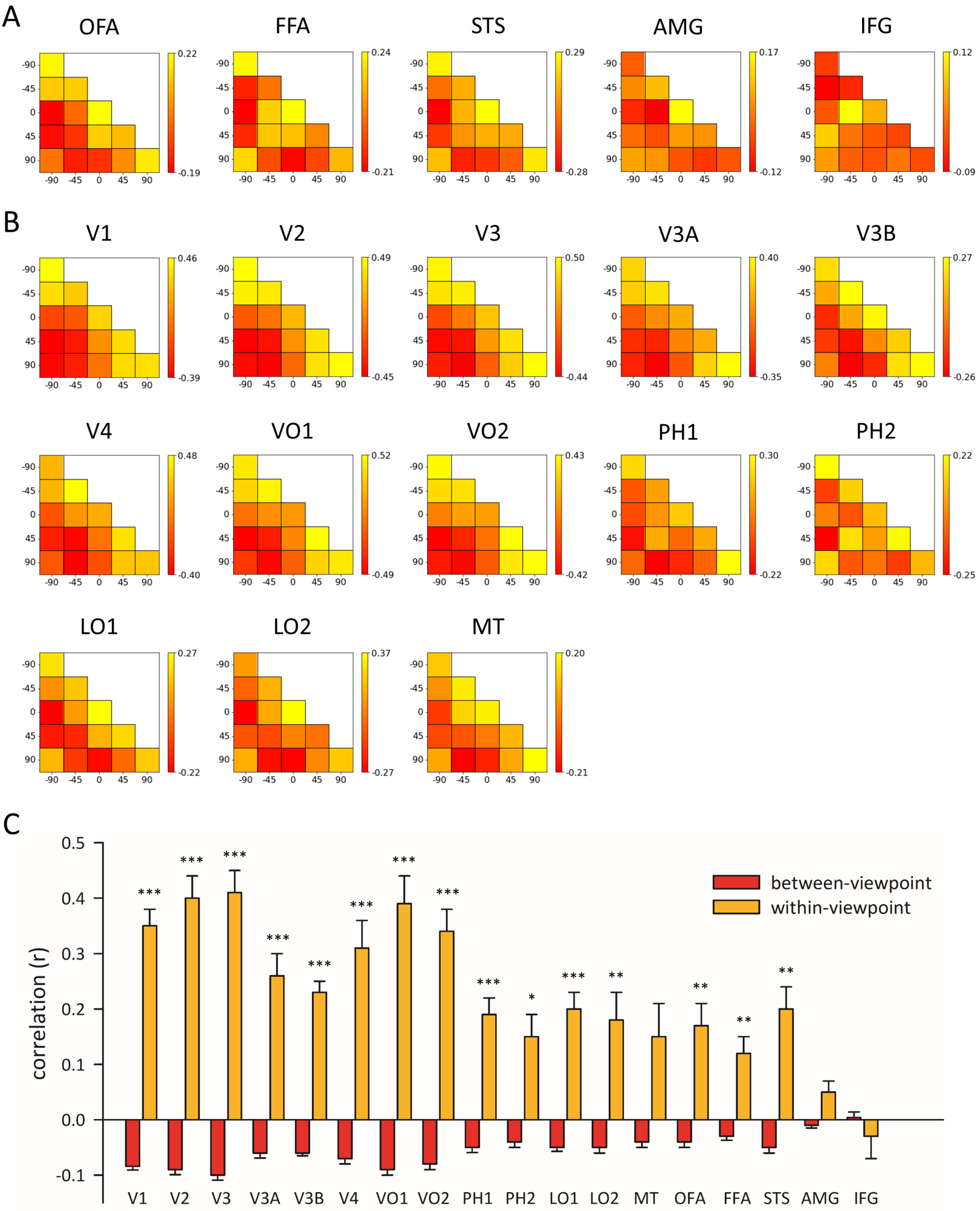
A
OFA
FFA
STS
AMG
IFG
B
V1
V2
V3
V3A
V3B
V4
VO1
VO2
PH1
PH2
LO1
LO2
MT
C
correlation (r)
between-viewpoint
within-viewpoint
V1 V2 V3 V3A V3B V4 VO1 VO2 PH1 PH2 LO1 LO2 MT OFA FFA STS AMG IFG

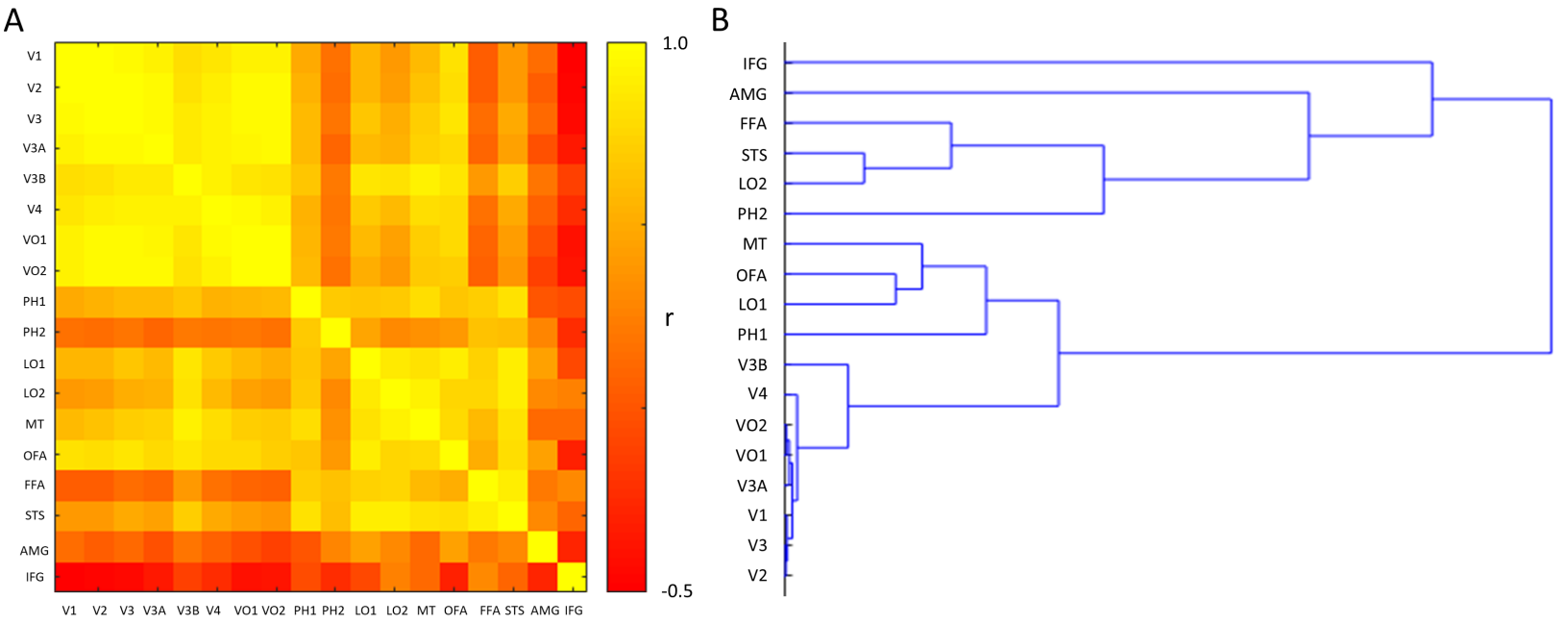
A
V1
V2
V3
V3A
V3B
V4
VO1
VO2
PH1
PH2
LO1
LO2
MT
OFA
FFA
STS
AMG
IFG
1.0
r
-0.5
B
IFG
AMG
FFA
STS
LO2
PH2
MT
OFA
LO1
PH1
V3B
V4
VO2
VO1
V3A
V1
V3
V2

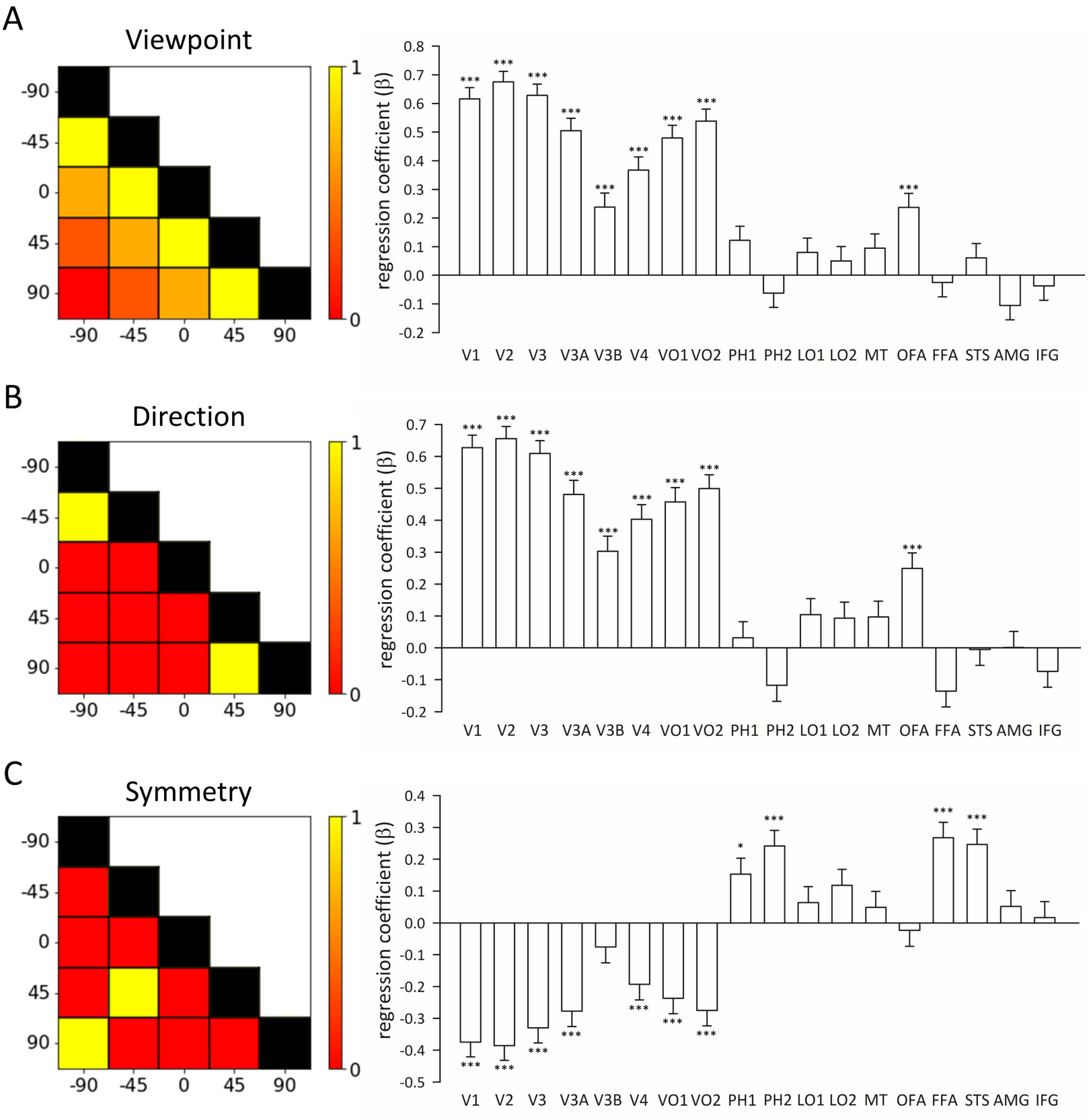
A
Viewpoint
B
Direction
C
Symmetry
-90
-45
0
45
90
1
0
regression coefficient (β)
V1 V2 V3 V3A V3B V4 VO1 VO2 PH1 PH2 LO1 LO2 MT OFA FFA STS AMG IFG

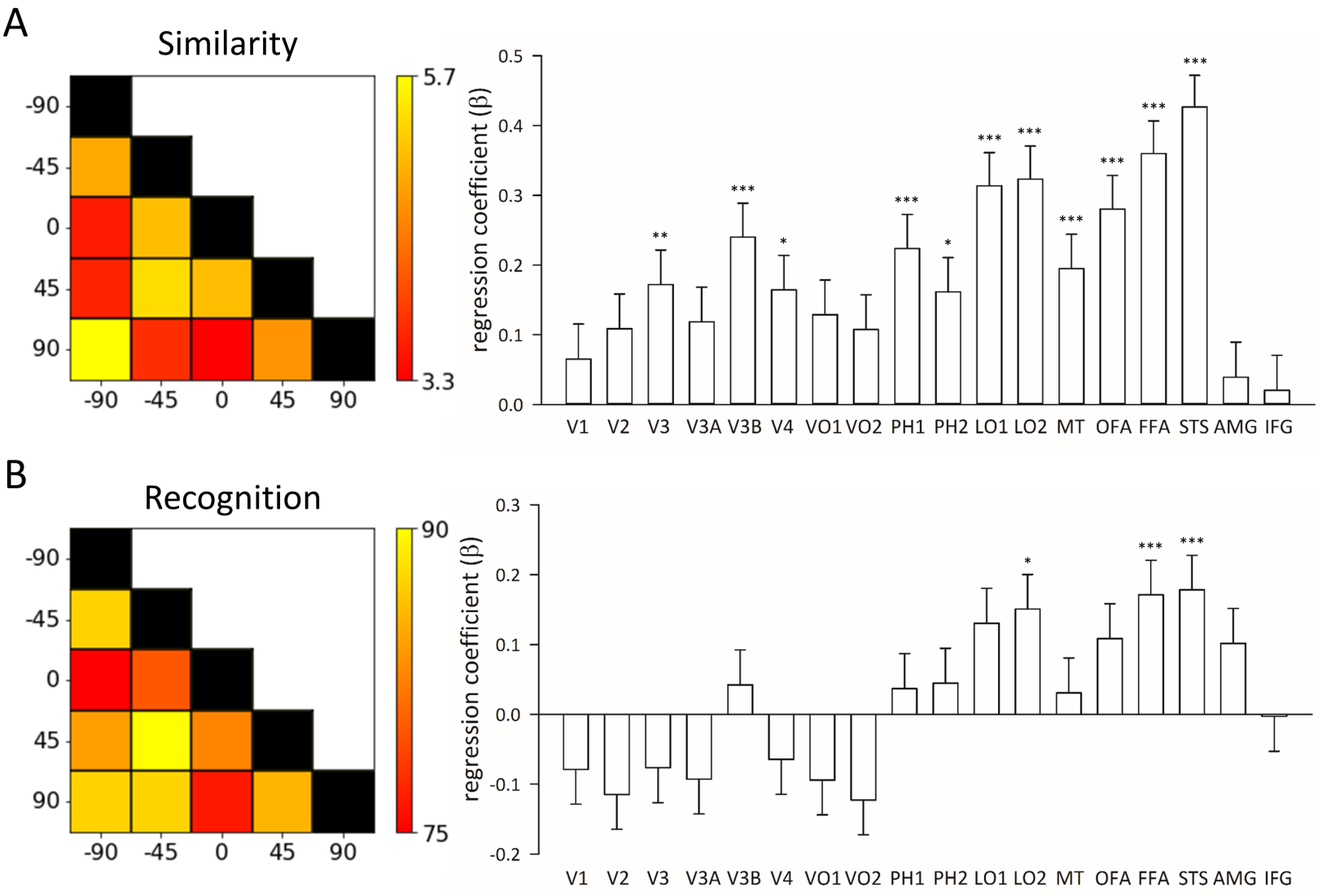
A
Similarity
-90
-45
0
45
90
5.7
3.3
regression coefficient (β)
0.5
0.4
0.3
0.2
0.1
0.0
V1 V2 V3 V3A V3B V4 VO1 VO2 PH1 PH2 LO1 LO2 MT OFA FFA STS AMG IFG
B
Recognition
90
75
-0.1
-0.2